Zero-Temperature-Coefficie AlN Epitaxial Films

著者	Tsubouchi Kazuo, Mikoshiba Nobuo
journal or publication title	IEEE Transactions on Sonics and Ultrasonics
volume	32
number	5
page range	634-644
year	1985
URL	http://hdl.handle.net/10097/47762

Zero-Temperature-Coefficient SAW Devices on AlN Epitaxial Films

KAZUO TSUBOUCHI AND NOBUO MIKOSHIBA, SENIOR MEMBER, IEEE

Abstract—**New thin-film technologies are required for integrating zero-temperature-coefficient surface-acoustic-wave (SAW) devices and "active" semiconductor devices into one chip, which should be called RF IC on a silicon on sapphire or Si substrate. AlN thin film has a potential use in SAW devices operating over the gigahertz range because of its high SAW velocity. Zero-temperature-coefficient SAW delay lines operating over 1 GHz using the AlN/sapphire combination have been fabricated. Recent works on the following are discussed: 1) material growth and evaluation of AlN material constants, 2) SAW propagation loss and dispersion vs. frequency and film thickness, 3) effects of AlN film qualities on the temperature coefficient of delay, 4) potential use for integration of RF circuit, and 5) the effect of temperature on the performance of SAW correlator.**

I. Introduction

OVER THE PAST few years there has been considerable interest in the development of surface-acoustic-wave (SAW) devices in high data-rate signal processing systems such as spread-spectrum communication (SSC). New thin-film technologies are required for integrating zero-temperature-coefficient SAW devices and active semiconductor devices into one chip. The one chip device will be fabricated on a silicon on sapphire (SOS) or Si substrate and should be called a new kind of radio frequency integrated circuit (RF IC).

For a wide-band signal processing device such as a convolver or correlator for SSC, a high-frequency and low-dispersion characteristic is required on the above one-chip monolithic structure. Furthermore, in order to obtain electronic functions such as convolution or correlation due to acoustoelectric effects, we need an electrically stable metal–insulator–semiconductor (MIS) structure, where the insulator should be a piezoelectric thin film.

On the other hand, in order to fabricate the one chip RF IC, it is required that the piezoelectric thin film, which has a large electromechanical coupling constant, should be grown selectively onto SAW device parts of the substrate and compatibly with silicon device fabrication process. The thickness of the piezoelectric film will be limited to less than about 3 μm because of the defocusing of micropatterns in photolithography.

AlN thin films have a potential use in SAW devices operating over the gigahertz frequency range because of its high SAW velocity. Until now, however, very few reports have appeared on the elastic and the piezoelectric constants and the temperature coefficient of delay (TCD) for surface acoustic waves on AlN films.

For a few years we have been studying single-crystal AlN films on sapphire (Al_2O_3) and silicon (Si) substrates obtained by epitaxial growth using metalorganic chemical vapor deposition (MO-CVD). We have succeeded in experimentally fabricating zero temperature coefficient SAW delay lines over 1 GHz on the AlN/Al_2O_3 combination.

In this paper our recent works on the AlN epitaxial films are reviewed and the potential advantages of the AlN film are discussed for the application to the one chip RF IC.

II. Epitaxial Growth and Evaluation of AlN Material Constants

Thin films of AlN have been grown by various methods, such as MO-CVD [1]–[7], sputtering [8]–[12], and molecular beam epitaxy [13]. The MO-CVD method will be used more extensively than others because it provides a great degree of control and reproducibility.

The schematic diagram of our MO-CVD apparatus is illuatrated in Fig. 1. The AlN films were grown by a chemical reaction of a trimethylaluminum vapor (TMA, $(CH_3)_3Al$) with ammonia gas (NH_3) on a substrate, which is heated with a SiC coated graphite susceptor by RF (20 kHz ~ 400 kHz) inductive heating.

A typical growth condition is shown in Table I. The film thickness was monitored by an interferometer consisting of a He–Ne laser as an *in situ* monitor. The growth rate of AlN film was typically 400 Å/min.

From Figs. 2–4, RED patterns and scanning electron microscope (SEM) micrographs of AlN films are shown [6], [14]. All the AlN films are about 1.0 μm thick. On basal plane sapphire ((0001)Al_2O_3), AlN films grew epitaxially above 1180°C with the orientation relationships: (0001)AlN//(0001)Al_2O_3 and $[\bar{2}110]$AlN//$[0\bar{1}10]$ Al_2O_3. On (111) plane silicon, AlN films grew epitaxially with the orientation relationships: (0001)AlN//(111)Si and $[11\bar{2}0]$AlN//$[1\bar{1}0]$Si above 1180°C, which was the same temperature as the (0001)AlN//(0001)Al_2O_3 case. On the other hand, on *R*-plane sapphire ($(1\bar{1}02)Al_2O_3$), AlN films grew expitaxially above 1005°C with the orientation relationships: $(11\bar{2}0)$AlN//$(1\bar{1}02)Al_2O_3$ and [0001]AlN// $[0\bar{1}11]Al_2O_3$.

The epitaxial-growth temperature on *R*-plane sapphire, where the *c*-axis of the AlN film is parallel to the substrate surface, is 1005°C; this is 175°C lower than the epitaxial-

Manuscript received August 5, 1984; revised January 10, 1985.

The authors are with the Research Institute of Electrical Communication, Tohoku University, Katahira 2-1-1, Sendai 980, Japan.

0018-9537/85/0900-0634$01.00 © 1985 IEEE

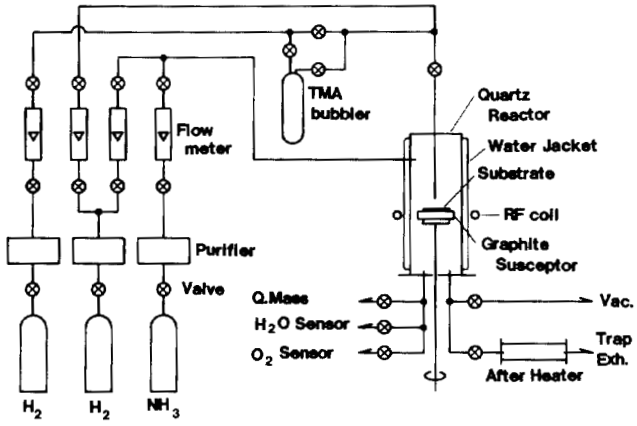

Fig. 1. Schematic diagram of MO-CVD.

TABLE I
GROWTH CONDITION OF AlN FILM

Growth temperature	1005°C – 1180°C
Bubbling H_2 flow rate	20 ml/min (TMA 1.2×10^{-5} mol/min at 25°C)
Back up H_2 flow rate	5.0 l/min
HN_3 flow rate	3.0 l/min
TMA nozzle—substrate distance	1.5 cm

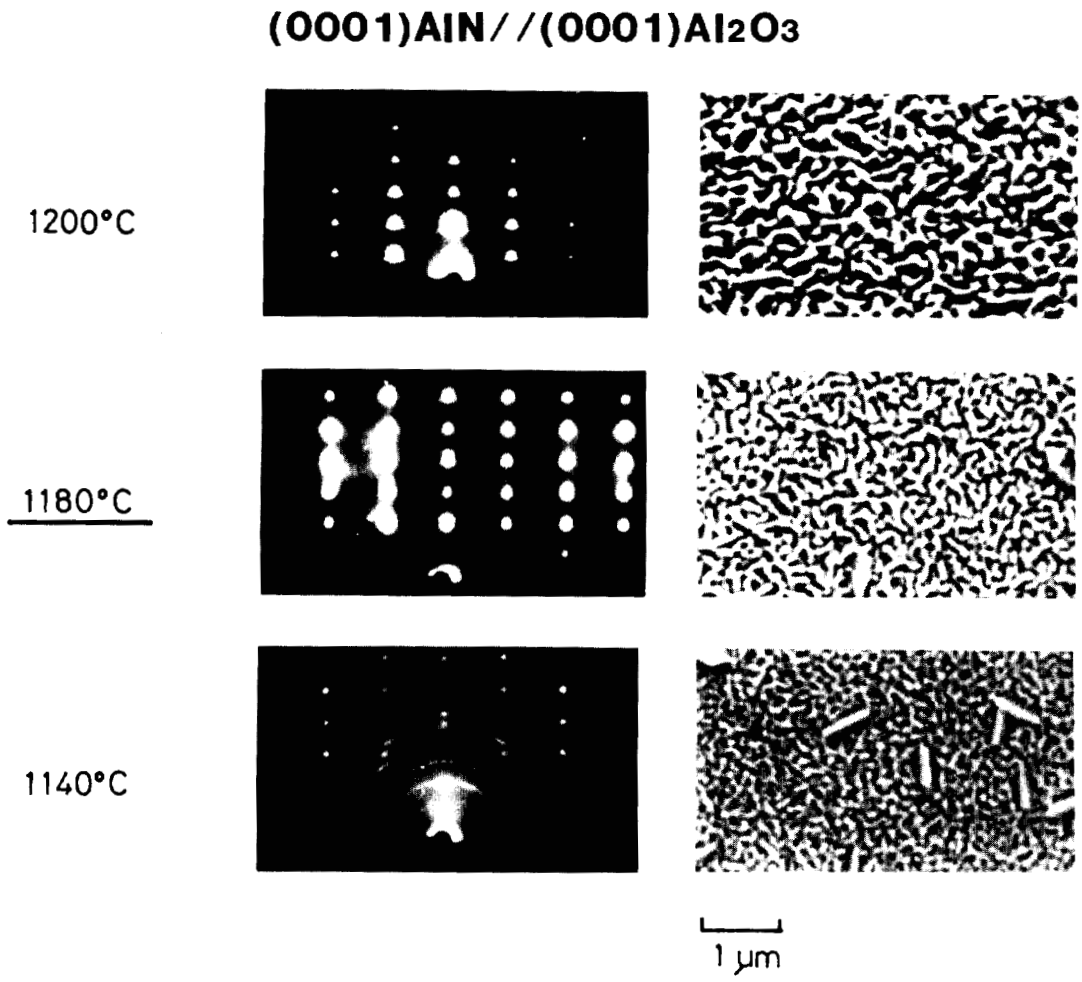

Fig. 2. RED patterns (left) and SEM micrographs (right) of AlN/(basal plane) Al_2O_3 at growth temperature T = 1200, 1180, and 1140°C, respectively.

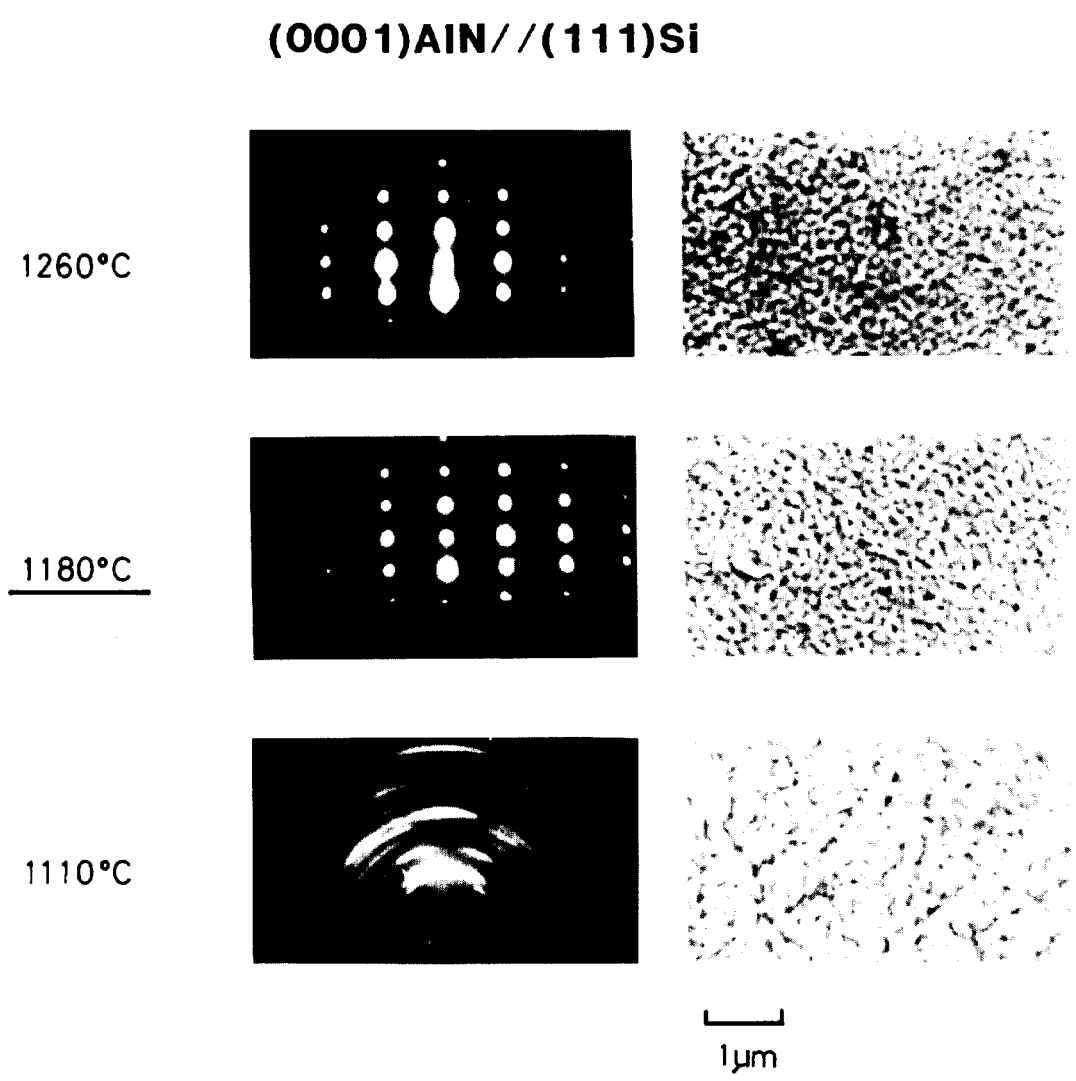

Fig. 3. RED patterns (left) and SEM micrographs (right) of AlN/(111)Si at growth temperature T = 1260, 1180, and 1110°C, respectively.

growth temperature where the c-axis of the AlN film is normal to the substrate surface.

For our device fabrication, we used only the single-crystal AlN films whose RED patterns showed individual spots.

Until now, elastic and the piezoelectric constants of AlN are not fully determined because a large-size bulk crystal has not been obtained. We have determined AlN material constants by computer fitting with experimental data of SAW characteristics on AlN films [15].

In order to determine the unknown constants of AlN, we assume Rayleigh-wave velocity v as a function of the unknown constants and the normalized film thickness kH of AlN films (where k is the wave number, and H is the film thickness), i.e.,

$$v = f(C_{11}^E, C_{12}^E, C_{13}^E, C_{33}^E, C_{44}^E, \epsilon_{11}^S, \epsilon_{33}^S, e_{15}, e_{31}, e_{13}, kH) \quad (1)$$

where C_{ij}^E, ϵ_{ij}^S, and e_{ij} are the stiffness constants, permittivity, and piezoelectric constants, respectively. The other known constants used in the calculation were the mass density of AlN; $\rho = 3.26 \times 10^3$ kg/m^3 [16], and the material constants of Al_2O_3 listed in the *Microwave Acoustic Handbook* [17].

The finding of AlN material constants was carried out by essentially trial and error many times to give an overall fitting of the calculated values with all the experimental data of phase velocity v and the coupling constants 2 $(\Delta v/v)$. The fitting results are shown in Figs. 5 and 6, where the previously reported experimental data on R-plane sapphire [2]–[5], [32] are shown as well as our data.

The material constants of AlN obtained by the computer fitting are

$$[C] = \begin{bmatrix} 3.45 & 1.25 & 1.20 & 0 & 0 & 0 \\ 1.25 & 3.45 & 1.20 & 0 & 0 & 0 \\ 1.20 & 1.20 & 3.95 & 0 & 0 & 0 \\ 0 & 0 & 0 & 1.18 & 0 & 0 \\ 0 & 0 & 0 & 0 & 1.18 & 0 \\ 0 & 0 & 0 & 0 & 0 & 1.10 \end{bmatrix} (10^{11}\ \mathrm{N/m^2})$$

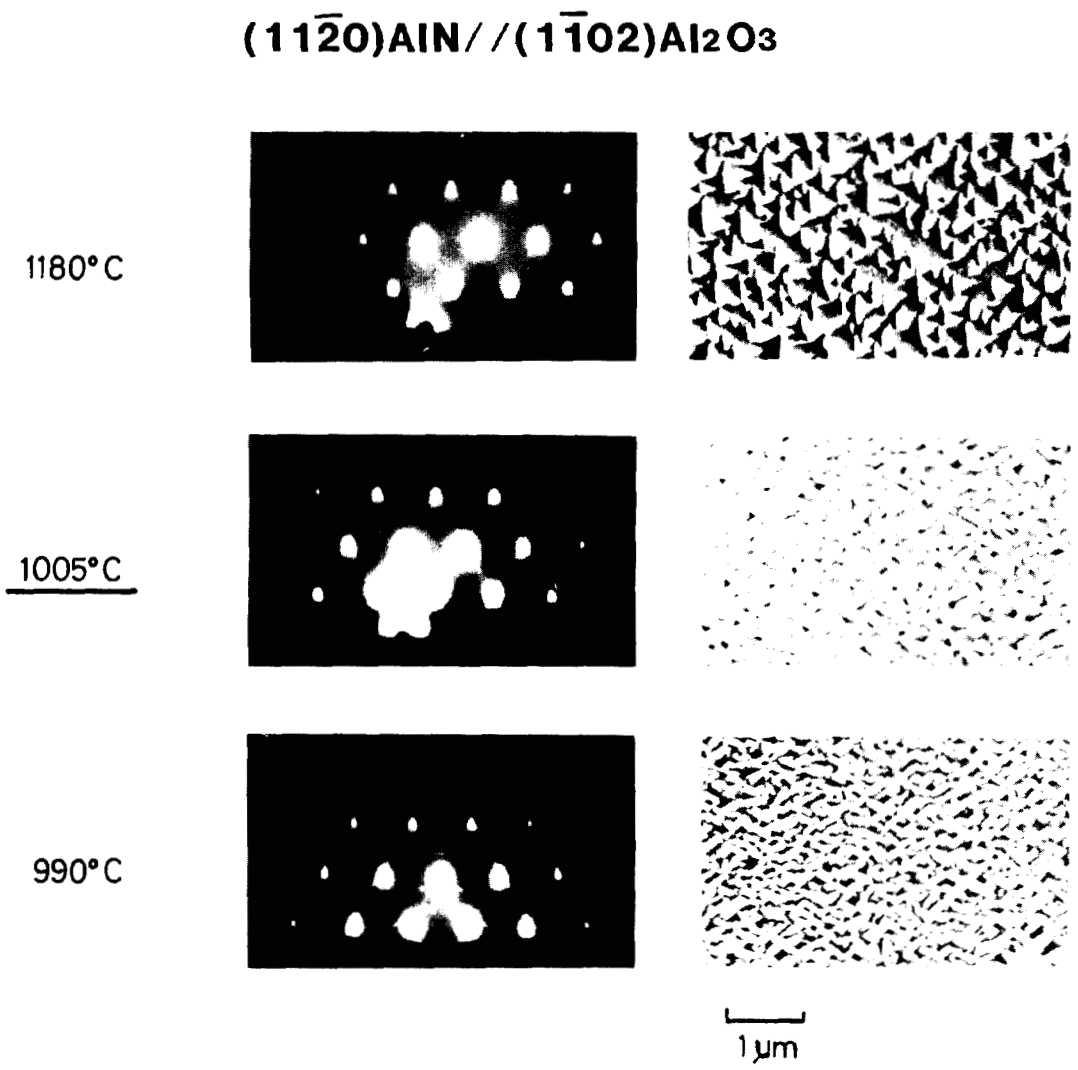

Fig. 4. RED patterns (left) and SEM micrographs (right) of AlN/(*R*-plane) Al_2O_3 at growth temperature T = 1180, 1005 and 990°C, respectively.

$$[e] = \begin{bmatrix} 0 & 0 & 0 & 0 & -0.48 & 0 \\ 0 & 0 & 0 & -0.48 & 0 & 0 \\ -0.58 & -0.58 & 1.55 & 0 & 0 & 0 \end{bmatrix} (\mathrm{C/m^2})$$

$$[\epsilon] = \begin{bmatrix} 8.0 & 0 & 0 \\ 0 & 8.0 & 0 \\ 0 & 0 & 9.5 \end{bmatrix} (10^{-11}\ \mathrm{F/m}).$$

The comparison between these values of AlN material constants by computer fitting and those reported previously are shown in Table II. Until now, only six components of material constants have been reported [18], [19] and a different set of constants was used. Therefore, we changed our set of constants for the comparison. The agreement between ours and others seems to be reasonable in view of the scattering of fitting experimental data. It is thought that the average error is within a few percent in our calculation.

We determined the sign of the piezoelectric constant d_{15} to be negative because a positive d_{15} caused an unreasonably small coupling constant $2(\Delta v/v)$, compared to the values of experimental data.

III. Zero-Temperature-Coefficient SAW Delay Line on AlN/Al_2O_3

Temperature stability is an important property in tapped-delay-line type SAW correlators, SAW resonators, SAW delay lines, and so on. Although Liu *et al.* [22] reported that AlN is expected to have a negative temperature coefficient of delay, Kagiwada *et al.* [5] later showed that it has a positive temperature coefficient of delay. Recently, Wang *et al.* [12] reported on low-temperature-coefficient bulk-acoustic-wave composite resonators with AlN/Si structures. We have investigated the temperature dependence of SAW propagation delay time on AlN films epitaxially grown on basal and *R*-plane sapphires.

Temperature coefficient of delay was determined by measuring a frequency change of a SAW delay line oscillator. The oscillation frequency was measured using an HP8568A spectrum analyzer. Only the SAW delay line was

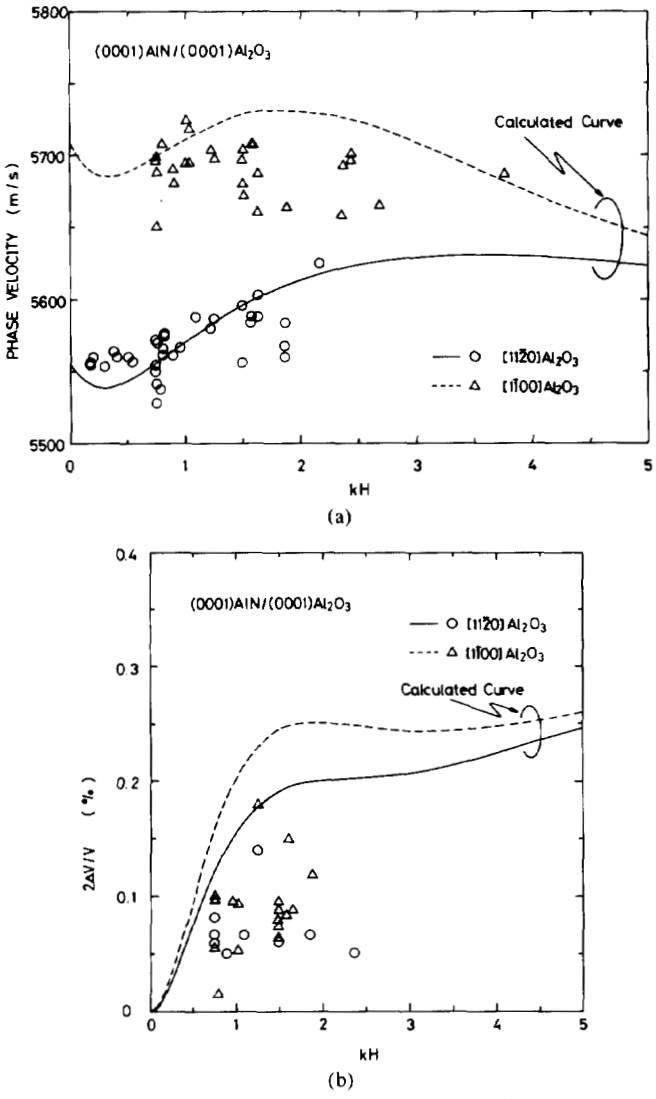

Fig. 5. Experimental data and calculated curves. (a) Phase velocities. (b) Coupling coefficients of Rayleigh waves on (0001) AlN/(0001) Al_2O_3.

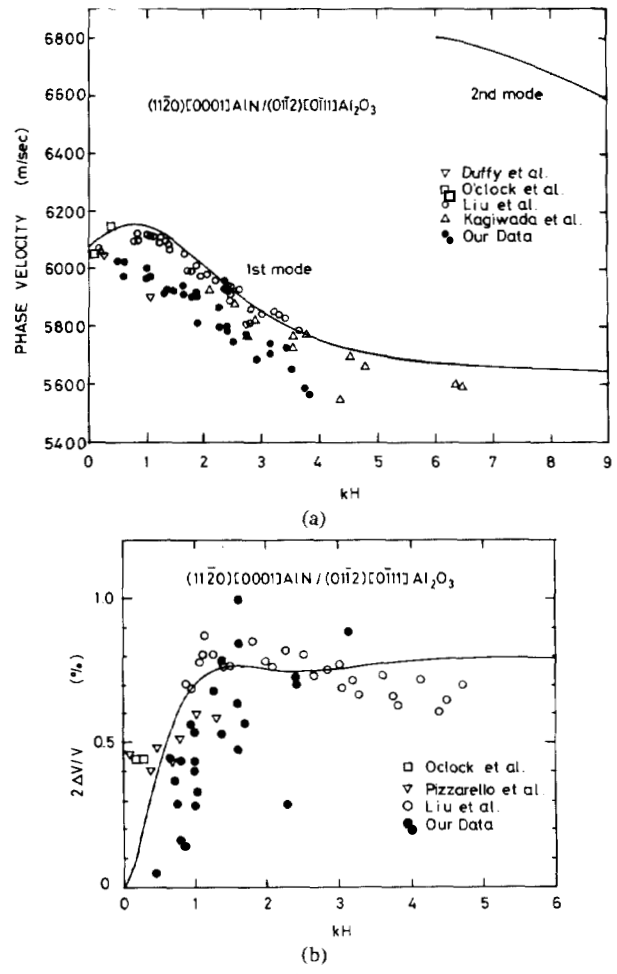

Fig. 6. Experimental data and calculated curves of Rayleigh waves on (11$\bar{2}$0) AlN (01$\bar{1}$2) Al_2O_3. (a) Phase velocities. (b) Coupling coefficients. The previously reported experimental data [2], [32], [3], [4], and [5] are shown with our data.

set in a thermostatic oven and its ambient temperature was changed from 0 to 50°C.

A temperature dependence of oscillation frequency of a (0001)AlN/(0001) [1$\bar{1}$00]Al_2O_3 SAW delay line oscillator is shown in Fig. 7. The direction of [1$\bar{1}$00] means the SAW propagation direction on the (0001)Al_2O_3 surface and the normalized thickness of the AlN film kH is 3.75. The actual thickness of the AlN film H was 3.0 μm and the pitch of the interdigital transducer (IDT) was 1.25 μm (= λ/4, λ; SAW wavelength). The oscillation frequency of 1.139 GHz was very stable throughout the temperature range, especially from 5 to 40°C [20].

In Fig. 8 the fractional frequency change $\Delta f/f_0$ of the oscillation frequency versus temperature is shown for the normalized AlN film thickness kH = 1.7, 2.3, and 3.0 on R-plane sapphire, respectively. The propagation direction of SAW was along the c-axis of AlN. When increasing the kH value from 2.3 to 3.0, the slope of the temperature dependence changed from negative to positive.

The variations of the measured TCD's at room temperature (25°C) with normalized AlN film thickness are shown in Fig. 9 for three kinds of AlN/Al_2O_3 combinations on R-plane and basal plane sapphire. It is evident that the TCD's for three kinds of AlN/Al_2O_3 combinations decreased with increasing kH and reached zero at kH = 2.7, 3.7, and 4.5 for (11$\bar{2}$0) [0001]A1N/(01$\bar{1}$2) [0$\bar{1}$11]Al_2O_3, (0001)AlN/(0001) [1$\bar{1}$00]Al_2O_3, and (0001)/AlN/(0001) [11$\bar{2}$0]Al_2O_3 combinations, respectively.

We have determined the temperature coefficients of the stiffness of AlN film by computer fitting using the exper-

TABLE II
COMPARISON BETWEEN THE PRESENT AND PREVIOUS MATERIAL CONSTANTS OF AlN

	Present Values	Values Reported previously	Reference
C_{11}^E (N/m^2)	3.95×10^{11}	4.04×10^{11}	[18]
C_{33}^D (N/m^2)	4.20×10^{11}	4.17×10^{11}	
S_{11}^E (m^2/N)	3.53×10^{-12}	3.30×10^{-12}	
ϵ_{33}^T	$12.0\ \epsilon_0$	$11.4\ \epsilon_0$	
d_{15} (C/N)	-4.07×10^{-12}	4×10^{-12}	[19]
d_{31} (C/N)	-2.65×10^{-12}	-2×10^{-12}	
d_{33} (C/N)	5.53×10^{-12}	5×10^{-12}	

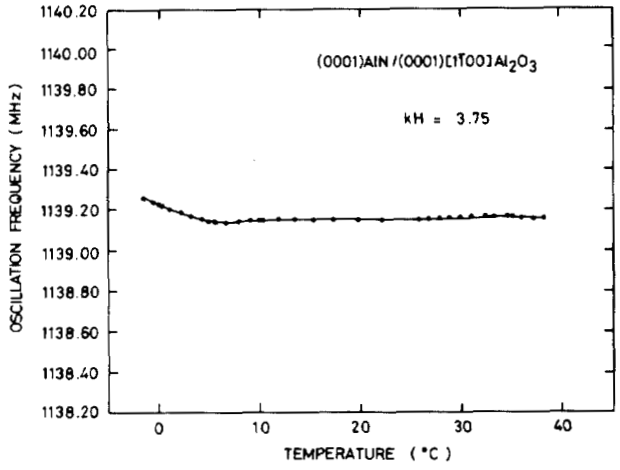

Fig. 7. Temperature dependence of oscillation frequency of AlN/basal-plane Al_2O_3 SAW delay-line oscillator of $kH = 3.75$.

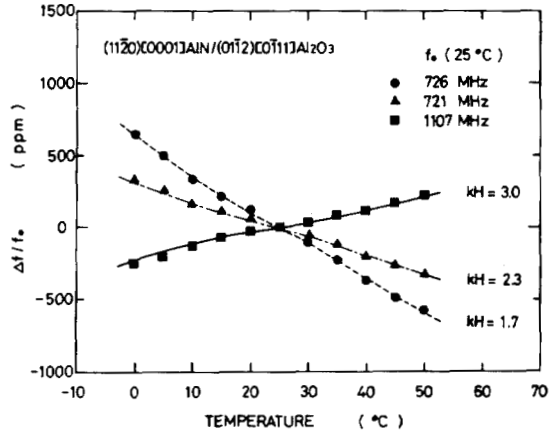

Fig. 8. Fractional frequency change $\Delta f/f_0$ of oscillation frequency versus temperature for AlN/R-plane Al_2O_3 SAW oscillators of $kH = 1.7$, 2.3 and 3.0, respectively.

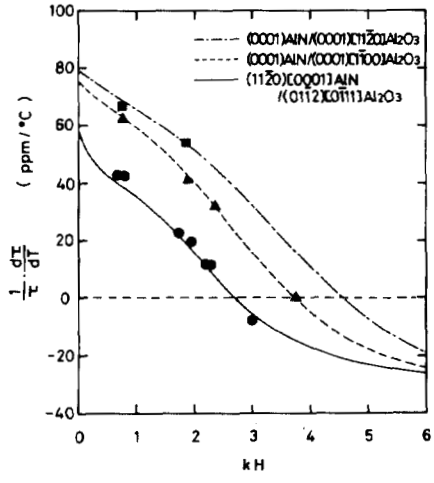

Fig. 9. TCD at 25°C vs. kH for three kinds of AlN/Al_2O_3 combinations on R-plane and basal plane sapphire and computer fitting curves.

imental data of AlN/Al_2O_3 combinations. TCD is approximated as follows

$$\mathrm{TCD} = \alpha - \mathrm{TCV} \tag{2}$$

where

TABLE III
MATERIAL CONSTANTS AND TEMPERATURE COEFFICIENT OF STIFFNESS TC (C^E) FOR AlN AND Al_2O_3

Material		AlN	Al_2O_3
ρ	(Kg/m^3)	3.26×10^3	3.98×10^3
C_{11}^E	(N/m^2)	3.45×10^{11}	4.97×10^{11}
C_{33}^E		3.95	4.98
C_{12}^E		1.25	1.64
C_{13}^E		1.20	1.11
C_{14}^E			−0.235
C_{44}^E		1.18	1.47
e_{31}	(C/m^2)	−0.58	
e_{33}		1.55	
e_{15}		−0.48	
ϵ_{11}^S	(F/m)	8.0×10^{-11}	8.28×10^{-11}
ϵ_{33}^S		9.5	10.2
α_{11}	(1/°C)	5.27×10^{-6}	7.28×10^{-6}
α_{33}		4.15	8.11
TC (C_{11}^E)	(1/°C)	0.8×10^{-4}	-0.75×10^{-4}
TC (C_{33}^E)		1.0	−0.85
TC (C_{12}^E)		1.8	0.40
TC (C_{13}^E)		1.6	−0.80
TC (C_{14}^E)			−0.70
TC (C_{44}^E)		0.5	−1.80
References		[15], [16], [29], [31]	[17], [29], [30]

$$\mathrm{TCV} = \frac{1}{v_s(25°\mathrm{C})}\left[\frac{v_s(35°\mathrm{C}) - v_s(15°\mathrm{C})}{20°\mathrm{C}}\right] \tag{3}$$

α is the thermal expansion coefficient along the SAW propagation direction, and v_s is the SAW phase velocity at each temperature. The computer calculation method for the layer structure was similar to that of [21]. The material constants used for the computer calculation are listed in Table III together with the temperature coefficient of stiffness constants TC(C_{ij}^E) for the AlN film.

From the experimental results and the theoretical evaluation for the SAW properties on our AlN films, we can conclude that single-crystal AlN has a negative TCD of about −30 ppm/°C, and it is expected to obtain a zero TCD by combination with appropriate positive TCD substrates.

IV. SAW Propagation Loss and Dispersion on AlN Films

Propagation loss and dispersion of SAW are also the important properties. We measured propagation loss of SAW on AlN films on sapphire substrates in the frequency range of 490 MHz and 1200 MHz by a laser probing method. The as-grown surfaces of AlN films grown at T ~ 1180°C were not smooth enough to fabricate IDT's on the surface, and they were polished slightly with 0.3-μm alumina powders. On the other hand, the as-grown surface at T ~ 1005°C and 990°C were smooth enough to fabricate IDT's but their films showed a higher loss than those of the polished surfaces and exhibited about a half value of the coupling constants of the films grown at T ~ 1180°C.

In Fig. 10, SAW propagation loss versus AlN film thick-

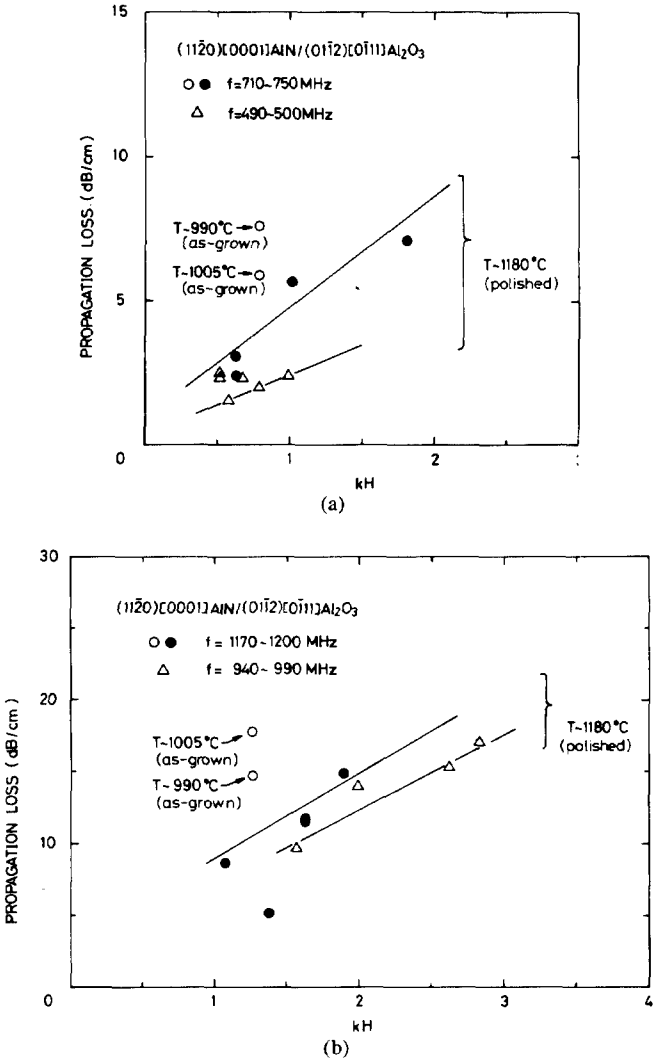

Fig. 10. Propagation loss of SAW versus AlN film thickness for AlN/*R*-plane sapphire in the frequency range. (a) 490 ~ 750 MHz. (b) 940 ~ 1200 MHz.

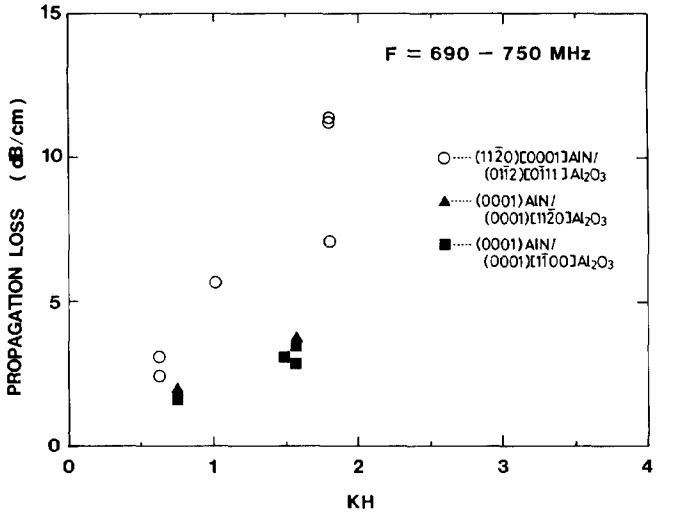

Fig. 11. Propagation loss of SAW versus AlN film thickness for AlN/basal-plane and *R*-plane sapphire in the frequency range of 690 MHz and 750 MHz.

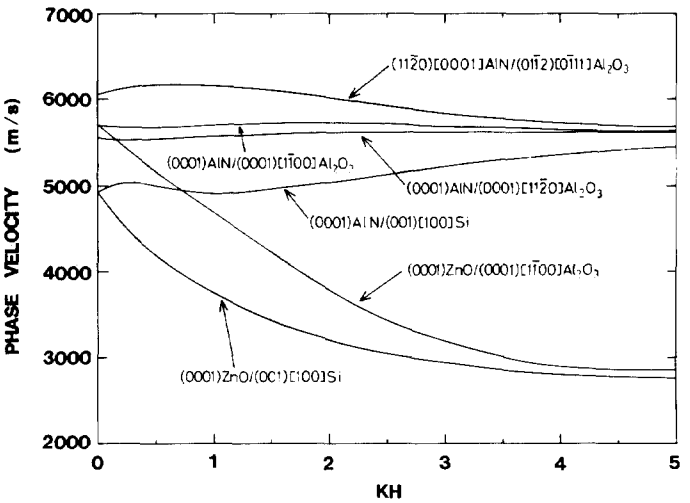

Fig. 12. Comparison of SAW dispersion curves for AlN/Al_2O_3, AlN/Si, ZnO/Al_2O_3, and ZnO/Si combinations.

ness on *R*-plane sapphire is shown with frequency as a parameter. When increasing the thickness of AlN film, the SAW propagation loss is increased. The propagation loss on our AlN films seems to be due to surface roughness and defects in the film.

In Fig. 11, propagation loss of SAW versus AlN film thickness is shown for AlN/basal plane and *R*-plane sapphire in the frequency range of 690 MHz and 750 MHz. The propagation loss on AlN/basal-plane sapphire is much lower than that of AlN/*R*-plane sapphire. The reason seems due to the difference of the quality of the grown AlN film.

Using the obtained material constants of AlN, we calculated the phase velocity dispersion versus film thickness of AlN on sapphire and silicon substrates. The results are shown in Fig. 12. We compare SAW dispersion curves for AlN/Al_2O_3, AlN/Si, ZnO/Al_2O_3, and ZnO/Si combinations. Comparing with the ZnO film, the AlN films show high-frequency and low-dispersion characteristics in SAW propagation, because of the AlN's high SAW velocity. The lowest dispersion curve is obtained for (0001)AlN/(0001) [11$\bar{2}$0]Al_2O_3 combination, although the coupling constant is about 0.2 percent as shown in Fig. 5. In the case of AlN/*R*-plane sapphire, i.e. (11$\bar{2}$0) [0001]AlN/(01$\bar{1}$2) [0$\bar{1}$11]Al_2O_3 combination, we can obtain a low-dispersion curve in conjunction with a moderate coupling of about 0.8 percent as shown in Fig. 6.

V. Qualities and Reproducibilities of AlN Films

We have tested electrical properties of AlN films [23]–[25]. As shown in Figs. 13–15, we have already demonstrated that a MIS structure of Al/AlN/Si is a useful material combination. AlN film seems to be a good electrical insulating layer (resistivity ~ 10^{16} Ωcm, breakdown field ≥ 10^6 V/cm), a good passivation layer (the interface state density ~ 10^{11} eV^{-1} cm^{-2}, the electron capture cross section ~ 10^{-17} cm^2) as well as a good piezoelectric layer. In order to obtain electronic functions such as convolution and correlation due to acoustoelectric effects, it is possible to use the nonlinear capacitance of the metal/AlN/Si

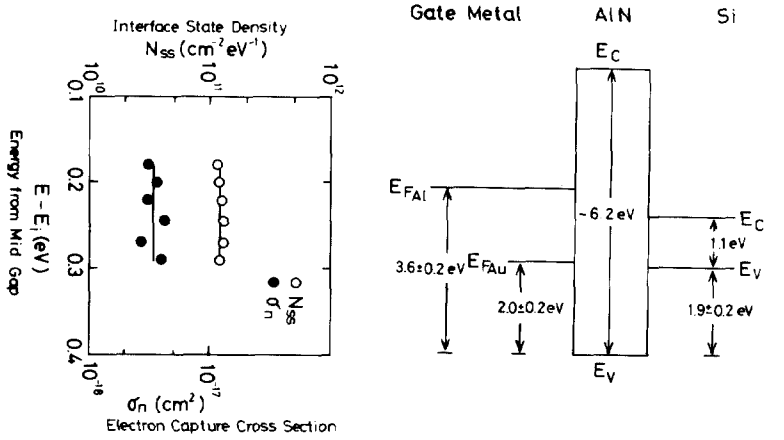

Fig. 13. Energy band diagram for MIS structure; metal/AlN/Si.

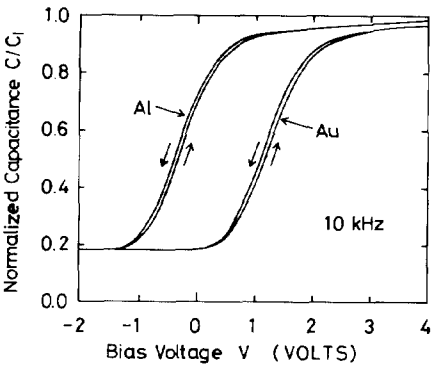

Fig. 14. Capacitance vs. field plate bias of metal/AlN/Si structures for two metal electrodes.

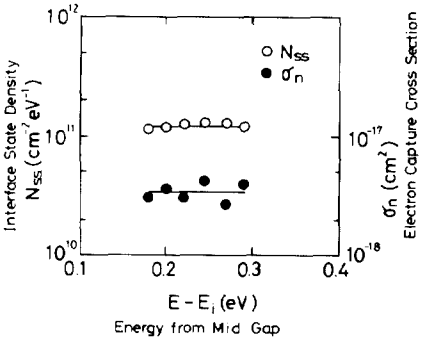

Fig. 15. Interface state density N_{ss} and electron capture cross section σ_n of interface states at AlN/Si.

structure in a future monolithic SAW device on a silicon and SOS substrate.

When we consider a fabrication process for SAW devices on AlN films grown by MO-CVD in the UHF frequency range, a big problem is the surface morphology of as-grown films. The hillock-like surface morphology as shown in Figs. 2–5 is not smooth enough to fabricate an IDT of pitch less than 3 μm by photolithography, while also causing large SAW propagation loss in the gigahertz range.

Very recently, a quite smooth-surface morphology of as-grown AlN film on (111)Si substrate was reported from a group of Clarion Co. Ltd. [26] as shown in Fig. 16. Its RHEED pattern showed streak lines which meant that the AlN film was a more perfect single-crystal film than those in Figs. 2–4. Therefore, it is worthwhile to find out the best growth condition which gives a smooth surface morphology of as-grown film.

The next problem is the reproducibility of the AlN film which give a zero TCD. In Fig. 17, TCD values at 25°C are shown for many our AlN films on *R*-plane sapphire substrates together with the data previously reported by Liu *et al.* [22], Kagiwada *et al.* [5], and Hurlburt [27]. There is a big scattering in the TCD values. Some TCD values of our AlN films are very similar to those previously reported by Liu *et al.* and Kagiwada *et al.*

The main reasons for such a big scattering in TCD would be due to some differences of AlN film qualities: 1) single-crystal film or poly-crystal film, 2) oxygen content, and 3) strain in the film.

We used only the single-crystal AlN films whose RED patterns showed individual spots. From our experimental data on the precise values of lattice constants of AlN films, which will give some information about strain in the film, it seems that there is no obvious correlation between the lattice constants and the TCD values.

On the other hand, as shown in Fig. 18, there is a tendency of correlation between the TCD values and the residual oxygen values which were determined by Auger electron spectroscopy (AES). The group of the AlN film, in which the oxygen content was from three to four percent showed the rapid decrease of TCD value with the increase of the thickness of AlN film and crossed a zero TCD value. The absolute value of the oxygen content by AES is not reliable because the AlN samples were set in the atmosphere. Another ambiguity is that the oxygen atoms will induce crystalline defects in the film and there will be complicated phenomena between oxygen content and crystalline imperfection.

At the present time, it could be suggested that there is a tendency for correlation between a zero TCD value and the oxygen content.

VI. Potential of AlN Film for One-Chip RF IC

Extending the performance of SAW devices requires an integration of acoustic and electric functions into a mo-

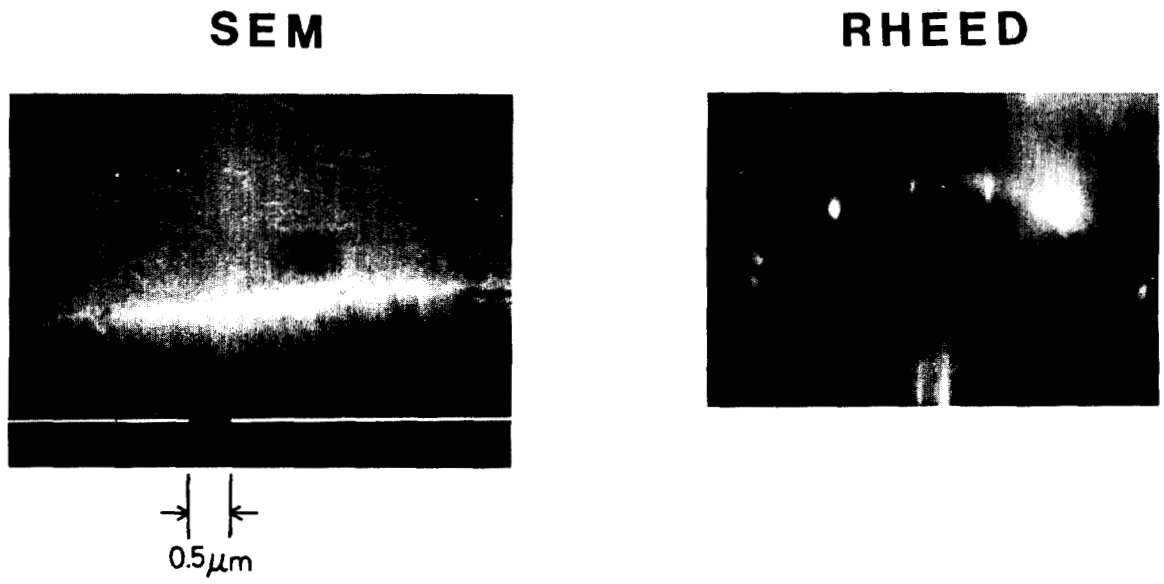

Fig. 16. Surface morphology and its RHEED pattern of as-grown AlN film on (111) Si [26].

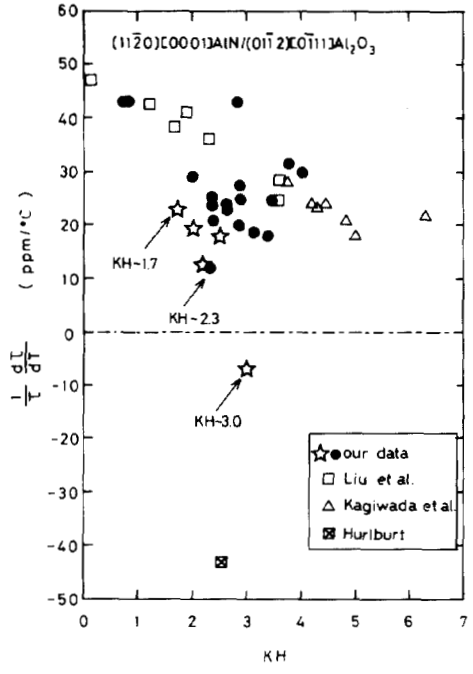

Fig. 17. TCD at 25°C vs. kH for AlN/R-plane sapphire combinations. The previously reported data of [22], [5], and [27] are shown as well as our data.

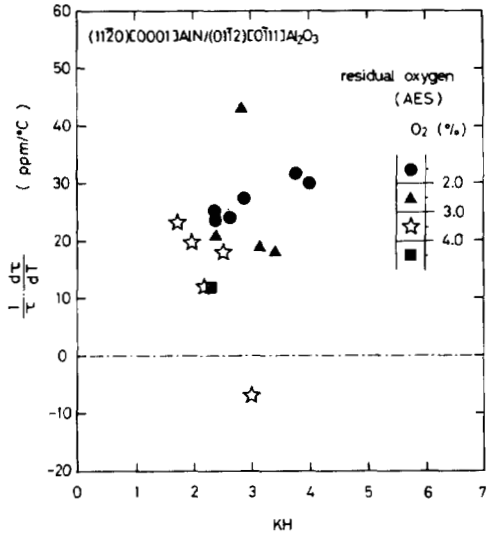

Fig. 18. Correlation between TCD and the oxygen content in AlN films for AlN/R-plane sapphire combination.

nolithic structure such as SAW devices on an SOS or Si substrate. AlN film has some potential advantages for the integration because of the possibility of integrating zero temperature coefficient SAW devices and active semiconductor devices into one chip on sapphire or silicon.

For example, a compact and mobile SSC transceiver needs the integration of SAW devices and semiconductor devices into one chip. One of the key devices in a SSC transceiver is a SAW correlator. For a wide band signal processing such as SSC, a large coupling constant for SAW generation is needed. The maximum bandwidth Δf is related to a coupling $2\Delta v/v$ as follows

$$(\Delta f/f_0) = \sqrt{4(2\Delta v/v)/\pi} \tag{4}$$

where f_0 is the center frequency. In the case of AlN/R-plane sapphire, we can obtain $2\Delta v/v \sim 0.8$ percent and $(\Delta f/f_0) \sim 10$ percent, and for example, $\Delta f = 100$ MHz in the case of $f_0 = 1000$ MHz.

On the other hand, a simple SAW correlator is a tapped delay line correlator, but the performance of the correlator is strongly degraded due to a temperature change [28]. For example, a tapped delay line correlator with center frequency $f_0 = 1000$ MHz, code length $N = 255$ chips (time-bandwidth product = 510), code rate $f_c = 50$ MHz, TCD = 10 ppm/°C, and the length of SAW correlator = 30 mm, the correlation peak is degraded by 3 dB at the

temperature difference $\Delta T = 10$ °C and to zero at $\Delta T = 20$°C.

In order to pick up the full potential of AlN film, an example of RF IC in the gigahertz range is proposed in [14]. As shown in the schematic figure [14], the one-chip spread spectrum demodulator includes the temperature stable devices as SAW bandpass filters, SAW oscillators, SAW correlators and SAW delay lines, and the active Si devices of amplifiers, mixers, AGC circuits and so on, with AlN–SOS combination.

V. Summary

We have determined the material constants of AlN using epitaxial films grown by a metal-organic chemical vapor deposition on sapphire and silicon substrates. We have succeeded in experimentally fabricating zero temperature coefficient SAW delay lines on AlN/Al_2O_3 combination. We have also found that AlN has a negative temperature coefficient of delay for SAW propagation.

The reproducibility of zero temperature coefficient of delay for SAW propagation seems to depend on oxygen contamination in AlN film. The surface morphology of as-grown film which mainly gives a surface-acoustic-wave propagation loss will be controlled by a careful film-growth technique.

It could be concluded that AlN film is a prospective material for thin film SAW devices and has a high potential for a one-chip RF IC such as an integrated spread spectrum transceiver incorporating zero-temperature-coefficient SAW correlators. Much more study is necessary to realize the full potential of AlN films for a SAW-device-based RF IC.

Acknowledgment

The authors wish to thank Dr. K. Sugai for his collaboration throughout this work.

References

[1] H. M. Manasevit, F. M. Erdmann, and W. I. Simpson, "The use of metalorganics in the preparation of semiconductor materials," *J. Electrochem. Soc.*, vol. 118, pp. 1864–1868, 1971.

[2] M. T. Duffy, C. C. Wang, G. D. O'Clock, Jr., S. H. McFarlane III, and P. J. Zanzucchi, "Epitaxial growth and piezoelectric properties of AlN, GaN, and GaAs on sapphire or spinel," *J. Electron. Mater.*, vol. 2, pp. 359–372, 1973.

[3] J. K. Liu, K. M. Lakin, and K. L. Wang, "Growth morphology and surface-acoustic-wave measurements of AlN films on sapphire," *J. Appl. Phys.*, vol. 46, pp. 3703–3706, 1975.

[4] F. A. Pizzarello and J. E. Coker, "The structureal and piezoelectric properties of epitaxial AlN on Al_2O_3," *J. Electron. Mater.*, vol. 4, pp. 25–36, 1975.

[5] R. S. Kagiwada, K. H. Yen, and K. F. Lau, "High-frequency SAW devices on AlN/Al_2O_3," in *Proc. 1978 IEEE Ultrasonic. Symp.*, 1978, pp. 598–601.

[6] M. Morita, N. Uesugi, S. Isogai, K. Tsubouchi, and N. Mikoshiba, "Epitaxial growth of aluminum nitride on sapphire using metalorganic chemical vapor deposition," *J. Appl. Phys. Japan*, vol. 20, pp. 17–23, 1981.

[7] M. Morita, S. Isogai, N. Shimizu, K. Tsubouchi, and N. Mikoshiba, "Aluminum nitride epitaxially grown on silicon: Orientation relationships." *J. Appl. Phys. Japan*, vol. 20, pp. L173–L175, 1981.

[8] A. J. Shuskus, T. M. Reeder, and E. L. Paradis, "RF-sputtered aluminum nitride films on sapphire," *Appl. Phys. Lett.*, vol. 24, pp. L155–L156, 1974.

[9] T. Shiosaki, T. Yamamoto, T. Oda, and A. Kawabata, "Low-temperature growth of piezoelectric AlN film by RF reactive planar magnetron sputtering," *Appl. Phys. Lett.*, vol. 36, pp. L643–L645, 1980.

[10] L. G. Pearce, R. L. Gunshor, and P. F. Pierret, "Aluminum nitride on silicon surface acoustic wave devices," *Appl. Phys. Lett.*, vol. 39, pp. L878–L879, 1981.

[11] S. Onishi, M. Eschwei, S. Bielaczy, and W. C. Wang, "Colorless, transparent, *c*-oriented aluminum nitride films grown at low temperature by a modified sputter gun," *Appl. Phys. Lett.*, vol. 39, pp. L643–L645, 1981.

[12] J. S. Wang and K. M. Lakin, "Low-temperature coefficient bulk acoustic wave composite resonators," *Appl. Phys. Lett.*, vol. 40, pp. L308–L310, 1982.

[13] S. Yoshida, S. Misawa, Y. Fujii, S. Takada, H. Hayakawa, S. Gonda, and A. Itoh, "Reactive molecular beam epitaxy of aluminum nitride," *J. Vac. Sci. Technol.*, vol. 16, pp. 990–993, 1979.

[14] K. Tsubouchi and N. Mikoshiba, "Zero-temperature-coefficient SAW delay line on AlN epitaxial films," in *Proc. 1983 IEEE Ultrason. Symp.*, 1983, pp. 299–310.

[15] K. Tsubouchi, K. Sugai, and N. Mikoshiba, "AlN material constants evaluation and SAW properties on AlN/Al_2O_3 and AlN/Si," in *Proc. 1981 IEEE Ultrason. Symp.*, 1981, pp. 375–380.

[16] K. M. Taylor and C. Lenie, "Some properties of aluminum nitride," *J. Electrochem. Soc.*, vol. 107, pp. 308–314, 1960.

[17] A. J. Slobodnik, Jr., E. D. Conway, and R. T. Delmonico, "Surface acoustic wave velocities," in *Microwave Acoustics Handbook*, vol. 1A. Air Force Cambridge Research Laboratory, Bedford, MA, no. TR-73-0597, 1973.

[18] T. Shiosaki, T. Yamamoto, T. Oda, K. Harada, and A. Kawabata, "Low-temperature growth of piezoelectric AlN film for surface and bulk wave transducer by RF reactive planar magnetron sputtering," in *Proc. 1980 IEEE Ultrason. Symp.*, 1980, pp. 451–454.

[19] A. R. Hutson, U.S. Patent, 3 090 876, May 21, 1963.

[20] K. Sugai, K. Tsubouchi, and N. Mikoshiba, "Zero-temperature coefficient surface-acoustic-wave delay lines on AlN/Al_2O_3," *J. Appl. Phys. Japan*, vol. 21, pp. L303–L304, 1982.

[21] S. Ono, K. Wasa, and S. Hayakawa, "Surface-acoustic-wave properties in $ZnO\text{-}SiO_2\text{-}Si$ layered structure," *Wave Electron.*, vol. 3, pp. 35–49, 1977.

[22] J. K. Liu, R. B. Stokes, and K. M. Lakin, "Evaluation of AlN films on sapphire for surface-acoustic-wave applications," in *Proc. 1975 IEEE Ultrason. Symp.*, 1975, pp. 234–237.

[23] M. Morita, S. Isogai, K. Tsubouchi, and N. Mikoshiba, "Characteristics of the metal insulator semiconductor structure: AlN/Si," *Appl. Phys. Lett.*, vol. 38, pp. 50–52, 1981.

[24] M. Morita, K. Tsubouchi, and N. Mikoshiba, "Interface barrier heights in metal-aluminum nitride-silicon structure by internal photoemission," *J. Appl. Phys.*, vol. 53, pp. 3694–3697, 1982.

[24] M. Morita, K. Tsubouchi, and N. Mikoshiba, "Electronic conduction in epitaxial aluminum nitride films on silicon," *J. Appl. Phys. Japan*, vol. 21, pp. 728–730, 1982.

[26] Y. Chubachi, K. Sato, and K. Kojima, "RHEED and X-ray studies of AlN films grown on (111)Si and (001)Si by MO-CVD," *Thin Solid Films.*, vol. 122, pp. 259–270, 1984.

[27] D. H. Hurlburt, *Heteroepitaxial Semiconductors for Electronic Devices*, G. W. Cullen and C. C. Wang, Ed. New York: Springer-Verlag, chap. 4, p. 174.

[28] P. H. Carr, P. A. Devito, and T. S. Szabo, "The effect of temperature and doppler shift on the performance of elastic surface wave encoders and decoders," *IEEE Trans. Sonics Ultrason.*, vol. SU-19, pp. 357–367, 1972.

[29] W. M. Yim and R. J. Paff, "Thermal expansion of AlN, sapphire, and silicon," *J. Appl. Phys.*, vol. 45, pp. 1456–1457, 1974.

[30] K. H. Hellwege, *Landolt-Börnstein Numerical Data and Functional Relationships in Science and Technology, New Series, Elastic, Piezoelectric and Related Constants of Crystal.* New York: Springer-Verlag, 1962.

[31] K. Tsubouchi, K. Sugai, and N. Mikoshiba, "Zero-temperature -coefficient surface-acoustic-wave devices using epitaxial AlN films," in *Proc. 1982 IEEE Ultrason. Symp.*, 1982, pp. 340–345.

[32] G. D. O'Clock, Jr., and M. T. Duffy, "Acoustic surface wave properties of epitaxially grown aluminum nitride and gallium nitride on sapphire," *Appl. Phys. Lett.*, vol. 23, pp. 55–56, 1973.

Nobuo Mikoshiba (M'68–SM'83) was born in Nagano Prefecture, Japan, on October 3, 1930. He received the B.S. and Ph.D. degrees in solid-state physics from Nagoya University, Nagoya, Japan, in 1953 and 1960, respectively.

He joined the Electrochemical Laboratory, Tokyo, Japan, in 1957, where he was engaged in research on physical acoustics and acoustoelectronic devices. From 1961 to 1963 he was a Research Associate at the Institute for the Study of Metals, University of Chicago, Chicago, IL. Since 1974 he has been a Professor in the Division of Acoustoelectronics, the Research Institute of Electrical Communication, Tohoku University, Sendai, Japan. He has been engaged in research on SAW convolvers, SAW image scanners, SAW parametric amplifiers and generators, surface acoustooptic devices, SAW charge transfer devices, acoustic DFB lasers, and photoacoustic spectroscopy in semiconductors.

Dr. Mikoshiba is a member of the Physical Society of Japan, the Japan Society of Applied Physics, the Institute of Electrical Engineering of Japan, the Institute of Electronics and Communication Engineers of Japan, the Acoustical Society of Japan, and the American Physical Society.

Kazuo Tsubouchi was born in Kyoto, Japan, on February 6, 1947. He received the B.S., M.S., and Ph.D. degrees in electronics engineering from Nagoya University, Japan, in 1969, 1971, and 1974, respectively.

Since 1974, he has been with Research Institute of Electrical Communication, Tohoku University, Japan, and now the Associate Professor of Acoustoelectronics Division. His current interest is in RF IC for mobile communication.

Dr. Tsubouchi is a member of the Japan Society of Applied Physics, the Institute of Electrical Engineers of Japan, and the Physical Society of Japan.